Reviews on Advanced Materials and Technologies, 2026, vol. 8, no. 4, pp. 201–209
DOI: 10.17586/2687-0568-2026-8-4-201-209

Mechanical Vibrations Modeling and Analysis in Bulk Gallium Oxide Crystal

D.A. Kalganov [1,2,*], V.V. Kaminskii [1], P.A. Bogdanov [1], D.I. Panov [1], D. A. Bauman [1]

[1] Institute of Advanced Data Transfer Systems, ITMO University, Kronverkskiy pr., 49, lit. A, St. Petersburg, 197101, Russia
[2] Laboratory of Diffraction Methods for Investigation of Real Crystal-Structures, Ioffe Institute, Politekhnicheskaya, 26, St. Petersburg, 194021, Russia

Article history

Received October 01, 2026
Received in revised form, October 29, 2026
Accepted October 30, 2026
Available online November 03, 2026

Abstract

This study focuses on the characterization of elastic properties of β-phase gallium oxide crystals by the finite element method and the composite oscillator technique. The representative values of the elastic constants were obtained by the generalized gradient approximation as follows: C_{11} = 250.4 GPa, C_{12} = 132.3 GPa, C_{13} = 148.8 GPa, C_{15} = –19.6 GPa, C_{22} = 357.1 GPa, C_{23} = 101.1 GPa, C_{25} = 16.4 GPa, C_{33} = 334.5 GPa, C_{35} = 4.5 GPa, C_{44} = 64.4 GPa, C_{46} = 27.2 GPa, C_{55} = 69.1 GPa, and C_{66} = 99.8 GPa. Room-temperature composite oscillator measurements gave a resonance frequency of 107954 Hz and a logarithmic decrement of $2.59 \cdot 10^{-4}$, in good agreement with the finite-element prediction of a longitudinal resonance near 108624 Hz and with the assumed loss factor. These results provide the scientific benchmark for studying elasticity and microplasticity of β-Ga_2O_3 by acoustic resonance techniques.

Keywords: Elastic properties; Piezoelectric composite oscillator technique; Density functional theory; Finite element method; Gallium oxide

1. INTRODUCTION

Gallium oxide is currently attracting considerable attention as a promising candidate for replacing silicon in power electronics, competing with other emerging semiconductor materials such as aluminum nitride, silicon carbide, and diamond. Among the five known polymorphs of gallium oxide, monoclinic beta-phase (β-Ga_2O_3) is the most thermodynamically stable phase over the entire temperature range up to its melting point (approximately 1800 °C). The other forms are metastable and transform into the beta phase upon heating above 750 to 900 °C. Studies of the monoclinic beta phase are the most numerous, owing, on the one hand, to its unique stability and, on the other hand, to the complexity of its properties associated with the low symmetry of its crystal structure [1,2].

A standard approach for determining the elastic constants and engineering moduli of solids, and of β-Ga_2O_3 in particular, is the iterative refinement of reference values obtained by density functional theory or molecular dynamics methods, using indirect experimental measurements of these quantities [3–6]. Owing to the complex crystal structure of β-Ga_2O_3 and the strong anisotropy of its properties, the number of independent parameters associated with experimentally measured quantities is large. Consequently, it typically requires complementary methods to evaluate these parameters and to determine the additional relationships among them [7]. The standard and most widely employed exchange-correlation functional for calculating the mechanical properties of oxides is the generalized gradient approximation in the Perdew-Burke-Ernzerhof formulation (GGA-PBE). Numerous studies have demonstrated that, for elastic constants, GGA-PBE yields an accuracy comparable to experimental measurements (with deviations of 5–15%), which is sufficient to utilize the derived values as reliable reference data. In contrast, while hybrid functionals provide a more accurate description of the bandgap, they yield only marginal improvements in the predicted elastic properties at a substantially higher computational cost. For instance, it has been shown in Ref. [7]

* Corresponding author: D.A. Kalganov, e-mail: kalganov@itmo.ru

© 2026 ITMO University. This is an open access article under the terms of the CC BY-NC 4.0 license.

that local density approximation (LDA) calculations reproduce the experimental C_{ij} with high accuracy, whereas hybrid functionals offer no systematic advantage for determining elastic constants. Crucially, the inherent band-gap underestimation characteristic of GGA-PBE does not directly affect the curvature of the potential energy surface in strain space. Furthermore, this approach significantly reduces the computational overhead and holds considerable promise within the delta-learning paradigm for refining results via machine-learned interatomic potentials [8].

Resonant ultrasound spectroscopy (RUS) studies [3] have shown the feasibility of identifying resonance modes in bulk gallium oxide single crystals using laser-Doppler interferometry. The RUS method is generally effective for anisotropic materials of high-symmetry crystal systems up to orthorhombic. However, the identification of several resonance types based on the displacement distribution in the sample [3,9] has enabled the corresponding deformation mode to be determined and the elastic constants to be evaluated. Because the RUS method requires free-vibration conditions for the most complete analysis of the spectrum of all vibrational modes, the contribution of internal damping to the quality factors of the relevant resonance peaks remains uncertain [10]. Moreover, this method offers limited capability to vary the amplitude of the vibrational strain and to detect nonlinear amplitude effects associated with microplasticity and anelasticity. Furthermore, a complete characterization of the full anisotropy of the mechanical quality factor Q, which reflects the dissipative properties of the material, has not been fully developed for RUS due to several fundamental limitations [10]:

– the linewidth of the resonance peaks in the vibration spectrum, from which Q is derived, depends on complex combinations of the elastic moduli;

– under conditions of high damping, the resonance peaks broaden and higher-order modes begin to overlap, making reliable measurements of the loss tangent (tan δ) feasible only for the fundamental (e.g., torsional) mode;

– incorporating the viscoelastic behavior of materials into the analytical framework significantly complicates RUS modeling and increases computational overhead, practically restricting the analysis to numerical solutions of vibration problems via the finite element method (FEM) [11,12];

– for low-symmetry crystals (such as monoclinic β-Ga_2O_3), peak splitting caused by pronounced elastic anisotropy and geometric imperfections of the sample further complicates spectral interpretation.

As an alternative to RUS, broadband viscoelastic spectroscopy can be employed; however, this technique suffers from significant drawbacks, primarily related to the complexity of sample preparation and the difficulty of accurately interpreting torsional and bending strain states in non-orthotropic materials [10].

The piezoelectric ultrasonic composite oscillator technique (PUCOT), in contrast, allows excitation of fundamental or harmonic longitudinal modes [13,14] and investigation of the amplitude dependence of the damping decrement and the effective elastic modulus, including single crystals of different lattice symmetries [15–17]. Owing to their common physical basis, RUS and PUCOT are complementary techniques well suited for studying material samples – especially those that are difficult to prepare, such as single crystals.

The use of PUCOT as an independent technique, or as a complement to RUS, enables the investigation of viscoelasticity, including nonlinear and microplastic effects. PUCOT data should make it possible to determine the remaining components of the elasticity and attenuation tensors by combining the elastic constants obtained from RUS and PUCOT with the corresponding direction-dependent attenuation components.

This work aims to model the mechanical (acoustic) vibrations in bulk gallium oxide crystals, analogous to the PUCOT technique employed in our study, in order to ensure the following conditions:

– unambiguous identification of the vibration mode (the fundamental longitudinal mode in PUCOT);

– high measurement accuracy through the matching of the dynamic resonance frequencies of the constituent parts of the composite oscillator [15,18];

– the absence of resonance peak overlap (suppression of bending and torsional modes in PUCOT).

The numerical model of the sample was constructed within the framework of linear dynamics, involving a single vibrational mode (longitudinal L_{010}), in order to develop the methodology and assist in interpreting experimental acoustic spectroscopy data in future studies. The specific length of the samples under study was also chosen to satisfy the fundamental longitudinal resonance condition (L_{010} mode) in the frequency range of ~10^5 Hz, characteristic of the PUCOT setup, and is based on the typical dimensions of samples manufactured from available bulk β-Ga_2O_3 crystals (see Figure 1). The sample cross-sections were selected based on the crystallographic planes of β-Ga_2O_3, the practical capabilities for processing bulk material along these orientations, and the symmetry-based selection rules governing bending and torsional modes. Atomistic calculations of the elastic properties of β-Ga_2O_3 were performed by density functional theory using Quantum Espresso [19], and mechanical (acoustic) vibrations were modeled by the finite element method in COMSOL Multiphysics®. This approach provides validation for future studies employing a sequential refinement model of the elastic and dissipative properties of low-symmetry materials (bulk β-Ga_2O_3 crystals), based on calculations with significantly lower computational cost compared to existing techniques [3,7,11,12].

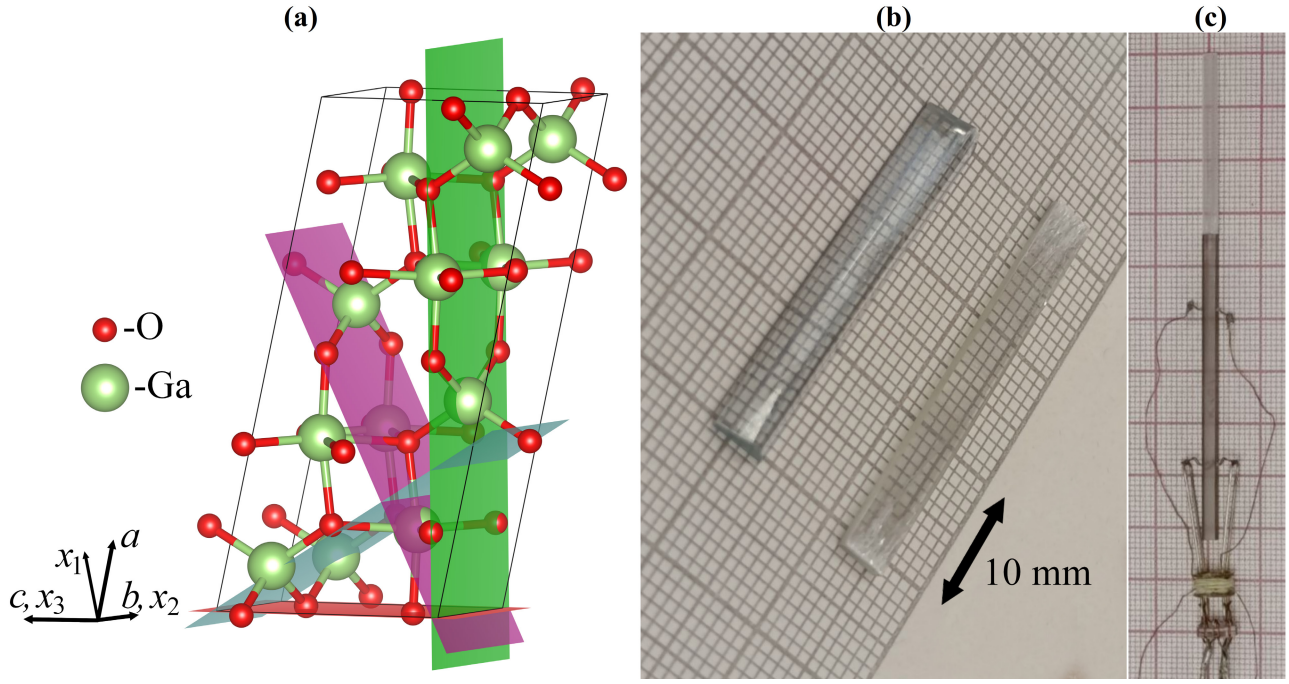


Fig. 1. Crystal lattice of β-Ga_2O_3: atoms, bonds, and slices by crystallographic planes of different orientations (a), bulk β-Ga_2O_3 crystals of rectangular and triangular cross-section (b), and triangular-cross-section sample mounted on the composite oscillator (c).

To validate the numerical benchmark, the finite-element results are compared with room-temperature (~300 K) PUCOT measurements performed on the triangular-cross-section sample using the procedure described in Refs. [15,18,20].

2. MODEL

2.1. Coordinate system and crystallographic configuration

Voigt notation is used for the numerical models. The symmetric stress and strain tensors are represented as six-component vectors, and the elastic-constant tensor C_{ij} is written as a 6×6 matrix in an orthonormal laboratory frame (x_1, x_2, x_3). This frame is attached to the monoclinic crystal by taking x_2 parallel to the crystallographic b axis and x_3 parallel to the c axis (see Figure 1a). The axis x_1 is normal to the bc plane and is therefore directed along the reciprocal-lattice vector a^*. The Voigt indices 11, 22, 33, 23, 13, and 12 correspond to this orthonormal frame. The crystal unit cell configuration of β-Ga_2O_3 was constructed based on available literature data [1,7] using the VESTA software package. Two sample cross-sections were investigated to analyze mode mixing and suppression effects. The rectangular cross-section sample was defined with transverse dimensions of 2.07×3.43 mm. The triangular cross-section sample was defined with side lengths of 4.45, 3.30, and 5.70 mm. Both configurations shared an identical longitudinal length of L = 31.25 mm. The chosen sample geometry, crystallographic orientation, and dimensions are also highly advantageous for subsequent experimental investigations [16].

2.2. Density functional theory calculations

Elastic constants were obtained within the GGA-PBE using two types of pseudopotentials from the PSlibrary: ultrasoft (US) and projector augmented wave (PAW) [19,21,22]. The US pseudopotentials (Ga.pbe-dn-rrkjus_psl.1.0.0.UPF, O.pbe-n-rrkjus_psl.1.0.0.UPF) were employed as the primary, computationally efficient set. The PAW pseudopotentials (Ga.pbe-dn-kjpaw_psl.1.0.0.UPF, O.pbe-n-kjpaw_psl.0.1.UPF) were used for comparison and verification of the US results, accounting for their differing pseudopotential hardness while maintaining an identical plane-wave cutoff energy. This comparison demonstrates the potential of utilizing these results within the delta-learning paradigm. For gallium, both sets explicitly include semi-core d electrons, which is essential for an accurate description of chemical bonding in β-Ga_2O_3.

The elastic constants were determined by the stress-strain method from the components of the strain tensor of the deformed crystal. The following convergence criteria were adopted: total energy to within $1.36 \cdot 10^{-7}$ eV/atom and forces to within $2.57 \cdot 10^{-4}$ eV/Å. Convergence was verified with respect to the cutoff energy (E_{cut} ~ 1224 eV) and the k-point mesh (the total energy change between the 6×18×12 and 8×24×16 k-dimension was less than $2.7 \cdot 10^{-3}$ eV/atom). The charge density and potential cutoff was set to four times

the wavefunction cutoff $E_{rho} = 4 \cdot E_{cut}$. With the specified parameters, full relaxation of the lattice parameters and internal atomic coordinates was performed prior to the calculation of C_{ij}, and the atomic coordinates were relaxed for each deformed structure as well. Broyden mixing with $\beta = 0.6$ was used to accelerate self-consistency [19].

Taking into account the monoclinic symmetry of β-Ga_2O_3, 13 independent strain types were considered with amplitudes $\delta = \pm 0.005, \pm 0.0075, \pm 0.01$ for uniaxial tension, simple shear, and combined deformations. After calculating the energy of the deformed structures, the system of equations $\sigma_i = C_{ij} \cdot \varepsilon_j$ was solved by the least-squares method.

2.3. Finite element model

The calculated elastic constants (GGA-US) were used as reference values for subsequent modeling of mechanical vibrations in bulk β-Ga_2O_3 crystals using the finite element method. The loss factor was specified from known PUCOT literature data for the corresponding wave propagation direction [16], adopting an isotropic approximation of $2.5 \cdot 10^{-4}$ (the anisotropy of attenuation can be investigated using this method by experimentally constructing internal friction curves in future studies). For developing a numerical model of bulk β-Ga_2O_3 crystals by the finite element method, the dimensions and shape of the samples presented in Figure 1b and the previously adopted system of axes x_1, x_2, x_3 were used. Within the framework of linear elasticity theory, regimes of free vibrations and a regime of coupled vibrations with excitation through the acoustic contact area, analogous to the PUCOT method, were investigated. When constructing the finite element model, an unstructured mesh based on tetrahedral and prismatic elements was used, obtained by sweeping a triangular mesh along the longitudinal axis. This approach ensured high element quality and computational efficiency. The frequencies of the resonance peaks were extracted by fitting the displacement spectrum with a Lorentzian function, which is the standard phenomenological model for describing damped harmonic oscillators near resonance. The maximum element size was determined by the need to describe geometric features, primarily the sharp corners of the triangular cross-section, and was set equal to 0.5 mm based on the smallest linear dimension and the sine of the triangle angle. This value is significantly smaller than the element size estimate based on the minimum phase velocity and the wave criterion, taking into account the C_{ij} values, density $\rho = 5950$ kg/m^3, and a maximum frequency of $f_{max} = 140$ kHz. The minimum element size was also bound from below to avoid the appearance of degenerate elements with poor conditioning. A convergence mesh study was also performed to verify the numerical stability of the resonance frequency prediction. By reducing the maximum element size for the triangular cross-section sample (most sensitive) from 0.5 mm to 0.4 mm, the total number of elements increased from approximately $3 \cdot 10^4$ to $6 \cdot 10^4$. The fitted resonance frequency shifted by only 10 Hz (relative change $\Delta f / f \sim 10^{-5}$, confirming that the discretization error is negligible for the purpose of mode identification and stress analysis.

The mechanical (acoustic) contact area was specified as a circular region $R = 0.5$ mm with a spring foundation of isotropic stiffness 10^3 N/m, chosen so that the rigid-body mode frequency of the sample mounting system is several orders of magnitude lower than the acoustic resonance. In addition, an added mass equal to the sample mass was introduced in this region. This assumption reflects the typical impedance-matching condition achieved during the tuning of compound piezoelectric oscillators, ensuring optimal energy transfer to the longitudinal mode [15,18].

The standard free-vibration model of COMSOL Multiphysics® was employed, based on the momentum balance (equations of motion) in the frequency domain, with the corresponding time derivative replaced by oscillation frequency. In this model, the differential equations of motion are reduced, by means of the Fourier transform, to a system of linear algebraic equations expressing the balance of inertial, elastic, and dissipative forces.

Forced harmonic vibrations of the sample were studied in the frequency range from 90 to 140 kHz under excitation by a concentrated harmonic force of 1 mN applied at the center of the acoustic contact area. The choice of the 1 mN force magnitude was dictated both by numerical necessity (load scaling) within the framework of linear elasticity theory, and by the subsequent estimate of the upper operational limit of strain amplitudes in the PUCOT setup, $\varepsilon_{max} \sim 10^{-4}$, corresponding to the stiffness C_{22} and stress levels of $\sigma \sim 10^8$ Pa.

In the local coordinate system (x_1, x_2, x_3), the following were analyzed: the x_2 component of the displacement s_m at the central point of the acoustic contact and the distribution of individual stresses most important for initiating dislocation motion along the crystal axis ([010], *b* axis) crossing this point.

3. EXPERIMENT

The triangular-cross-section sample was measured using a piezoelectric ultrasonic composite oscillator (Fig. 1c) at a temperature of approximately 300 K. The quartz resonator had a free resonance frequency $f_q = 105891.73$ Hz and an intrinsic logarithmic decrement $\delta_q = 8.48 \cdot 10^{-5}$.

Ten independent measurements with regluing of the sample were performed to reduce the effect of acoustic contact variability. The sample logarithmic decrement and resonance frequency associated with the longitudinal mode of the sample were corrected for the free quartz

Table 1. Comparison of elastic constants C_{ij} (given in GPa) of β-Ga_2O_3 obtained by the following methods: experiment (RUS [3]), calculation by local density approximation (LDA [7]), and generalized gradient approximation using projector augmented wave (GGA-PAW) and ultrasoft (GGA-US) pseudopotentials.

Method	C_{11}	C_{12}	C_{13}	C_{15}	C_{22}	C_{23}	C_{25}	C_{33}	C_{35}	C_{44}	C_{46}	C_{55}	C_{66}
RUS [3]	257.6	128	160	–1.6	343.8	70.9	0.4	347.4	1	47.8	5.6	88.6	104
LDA [7]	242	127	140	–17.7	360	90.3	12	355	7.7	58	19.7	69	97
GGA-PAW	249.5	130.4	84.8	–32.0	348.2	51.2	30.5	349	3.9	109.4	39.6	200.1	257.6
GGA-US	250.4	132.3	148.8	–19.6	357.1	101.1	16.4	334.5	4.5	64.4	27.2	69.1	99.8

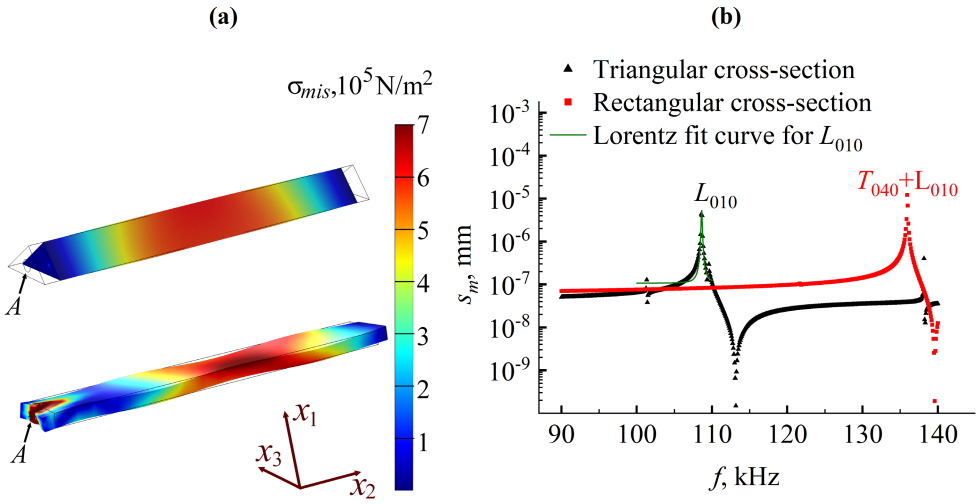


Fig. 2. Vibration model in bulk β-Ga_2O_3 crystals of rectangular and triangular cross-section. (a) distribution of equivalent stresses (von Mises stress) on the crystal surface (A – acoustic contact). The deformed shape and dimensional changes of the crystal at resonance are shown schematically with displacements magnified by a factor of 10^5. The original undeformed geometry is indicated by the empty-line contour. (b) frequency spectrum of displacement magnitude s_m (point A, x_2 axis – [010] direction).

frequency and intrinsic loss using the standard PUCOT relations [15,18,20]. Corresponding average values were $\delta = 2.6 \cdot 10^{-4}$ and $f = 107954$ Hz. For weak damping, the corresponding loss factor is $\eta = \delta/\pi \sim 8 \cdot 10^{-5}$, which is of the same order as the 10^{-4} adopted in the finite-element benchmark.

4. RESULTS AND DISCUSSION

The elastic constants obtained using ultrasoft (US) pseudopotentials show good agreement with experimental data [3] and first-principles calculations [7] for most diagonal components: C_{11}, C_{22}, C_{33}, as well as for the shear constant C_{66} and the off-diagonal constant C_{12}. The discrepancies for the shear constants C_{44} and C_{55} range from 20% to 35%, while the off-diagonal components C_{15}, C_{25}, C_{35}, and C_{46} in the US calculation are slightly overestimated compared with literature data. Such deviations are typical for GGA-PBE descriptions of shear responses in monoclinic systems and remain acceptable for providing a robust reference baseline for subsequent FEM analysis. The PAW calculation yields strongly overestimated shear constants C_{44}, C_{55}, C_{66}, and C_{13}, which makes it less preferable. A comparison of the obtained C_{ij} constants with literature data obtained in the same coordinate system is given in Table 1.

A parametric analysis of free vibration modes was performed by varying the constant C_{22}, which determines the stiffness along the crystallographic direction [010] (b axis), within ±10% (of the value from Table 1). The natural frequencies and shapes (modes) of free vibrations of the β-Ga_2O_3 crystal sample were determined, and the conditions for longitudinal resonance were identified at a frequency of about 108 kHz (Figure 2a).

In the forced vibration mode, for the rectangular cross-section sample (Figure 2b), the x_2 component of displacement (s_m) in the acoustic contact region is maximal upon excitation of mixed vibration modes along the corresponding axes: bending (B), torsional (T), and longitudinal (L), which is explained by the pronounced anisotropy of the mechanical properties of β-Ga_2O_3. The presence of mixed modes leads to errors in the experimental measurement of internal friction and Young's modulus. In the triangular cross-section sample (Figure 2b), the B and T modes are suppressed, which ensures that the vibration conditions correspond to the calculation methodology adopted in PUCOT and based on the longitudinal compliance of the material. Consequently, in the triangular

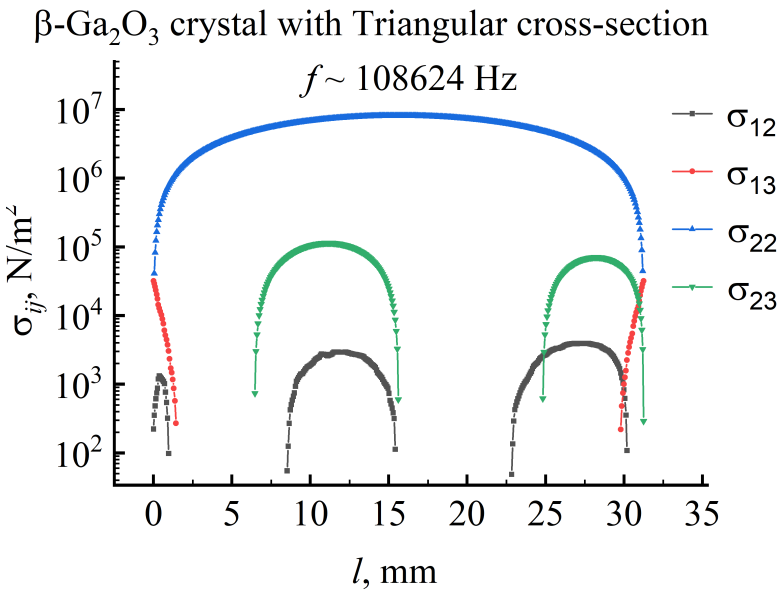


Fig. 3. Some components of the stress tensor along the x_2 axis over the sample length (from the acoustic contact point A; see Fig. 2).

cross-section configuration (specifically a scalene triangle lacking any mirror symmetry), *B* and *T* modes are effectively suppressed despite coupling mediated by off-diagonal elastic constants (C_{15}, C_{25}, etc.). The complete absence of symmetry elements prevents the formation of invariant subspaces that would otherwise allow coupling between longitudinal and bending/torsional degrees of freedom via off-diagonal elastic constants. This ensures a purely longitudinal response, which is essential for the correct interpretation of PUCOT data.

The PUCOT measurement provides a direct check of the finite-element benchmark. The calculated longitudinal resonance of the triangular sample is located near f_{calc} = 108624 Hz, whereas the room-temperature experiment gives f_{exp} = 107954 Hz. The residual difference is of order 7 Hz, corresponding to a relative discrepancy of approximately $6 \cdot 10^{-3}$. This agreement is within the combined uncertainty of the material parameters, sample geometry, and thermal corrections. The finite-element model used reference elastic constants without an explicit correction to the measurement temperature of ~300 K. The neglected temperature dependence of the elastic constants and thermal contraction of the crystal can also shift the resonance frequency by tens to hundreds of Hz [20]. Therefore, the observed difference between the calculated and measured resonance frequencies is attributable to the combined effect of density uncertainty, dimensional tolerance, and the missing temperature correction.

Some components of the stress tensor σ_{ij} in the crystallographic coordinate system are shown in Figure 3. In the fundamental approximation, its standing-wave pattern contains a single half-wave with a maximum at the center of the sample. For ideal free-type ends, σ_{22} vanishes at both end faces. However, at the acoustic-contact face this traction-free condition is not strictly satisfied, because the finite compliance of the spring foundation and the added mass replace the free-boundary condition with an elastic-support boundary condition. The shear and mixed stress components σ_{12}, σ_{23}, and σ_{13} are secondary with respect to the longitudinal mode: they are excited by elastic anisotropy, represented by the non-zero off-diagonal elastic constants C_{15}, C_{25}, C_{35}, and C_{46}, as well as by Poisson coupling between longitudinal and transverse strains. These components are proportional to derivatives of the transverse displacements u_1 and u_3, which in a three-dimensional resonant mode with a finite cross-section. Particularly in the presence of sharp corners of the triangular sample and boundary conditions on the lateral faces, that possess a more complex axial structure with several nodes of the stress field. Consequently, several half-waves of the standing-wave pattern appear as a jellyfish-like distribution of maxima on a logarithmic plot. Minimal values of the order of ~100 Pa correspond to the lower display threshold of the linear response to the applied 1 mN force at the nodes of the standing wave theoretical stresses vanish, which on a logarithmic scale manifest as termination of the curves rather than as a physical minimum.

Some components of the stress tensor of triangular cross-section crystal σ_{ij} (in the crystallographic coordinate system) are shown in Figure 3. The σ_{22} component is the primary normal stress of the L_{010} longitudinal mode and reaches ~10 MPa at the antinode of the standing wave once the resonant quality-factor amplification is included. Nevertheless, because the Burgers vector of the active $\langle 010 \rangle$ systems [23,24] coincides with the x_2 axis, σ_{22} does not enter the resolved shear stress (RSS) on any

slip plane containing [010]. The RSS on these systems is governed solely by the shear components σ_{12} and σ_{23} and does not exceed 1 MPa, i.e. three orders of magnitude below the critical resolved shear stress (CRSS) and three orders of magnitude below the ideal shear strength of the $\langle 010 \rangle / \{001\}$ system (3.9 GPa [23]). Consequently, dislocation glide is not activated under these excitation conditions, and the PUCOT response corresponds to reversible oscillation of dislocation segments between pinning points or local motion of dislocation segments in regions of high internal stress concentration in the crystal, similar to Ref. [25].

Comparisons with experimental acoustic spectroscopy data must account for differences in thermodynamic conditions (0 K in density functional theory calculations versus 300 K in experiments). As an example of a temperature coefficient for the elastic constants and moduli of crystals, relevant to the study of PUCOT, one can use data derived from an approximation of the corresponding relationship [20]. It should be noted, however, that this correction remains small compared to the uncertainties introduced by the choice of functional.

5. CONCLUSIONS

In the present work the elastic properties of bulk β-Ga_2O_3 crystals were investigated by combining density functional theory calculations with finite element analysis of mechanical vibrations. The GGA US pseudopotential approach yields elastic constants that agree well with experimental RUS [3] data for most diagonal components (C_{11}, C_{22}, C_{33}), the shear constant C_{66}, and the off-diagonal constant C_{12}, whereas the GGA PAW method strongly overestimates C_{44}, C_{55}, C_{66}, and C_{13}, making it less suitable for this material.

A parametric study of free vibration modes shows that the natural frequencies are sensitive to C_{22}, with longitudinal resonance near 108 kHz. Given the pronounced anisotropy of β-Ga_2O_3 monoclinic structure, the frequencies and mode mixing may depend on several diagonal and off-diagonal components of the elastic constant tensor C_{ij}. Consequently, a comprehensive sensitivity analysis remains necessary, employing the RUS technique and modeling the corresponding samples as small rectangular parallelepiped crystals in future. In the case of a sample with a rectangular cross-section, mixed modes can lead to errors in measurements of internal friction and Young's modulus by acoustic spectroscopy methods. In contrast, for a triangular cross-section in this crystallographic orientation, bending and torsional modes of crystal's vibration are suppressed, ensuring conditions consistent with the PUCOT methodology based on longitudinal compliance.

The calculated stress tensor components ($\sigma_{ij} < 10^8$ Pa) indicate that resolved shear stresses on dislocation slip systems remain two orders of magnitude below the critical one, so that only local motion of dislocation segments in regions of high internal stress concentration is possible for this excitation condition. This conclusion regarding dislocation motion and microplasticity was drawn taking into account the specific amplitude and acoustic contact characteristics employed and may be further refined in future work.

Room-temperature (~300 K) PUCOT measurements on the triangular sample yielded a resonance frequency of 107954 Hz and a logarithmic decrement of $2.593 \cdot 10^{-4}$. These values agree well with the finite-element prediction of a longitudinal resonance near 108 kHz and with the assumed isotropic loss factor of 10^{-4}. The small frequency discrepancy is attributable to the combined uncertainty in density, linear dimensions, and the neglected temperature correction of the elastic constants.

The obtained results provide a scientific benchmark for studying the elasticity and microplasticity of β-Ga_2O_3 by acoustic resonance techniques and are essential for strain engineering in electronic devices.

ACKNOWLEDGEMENTS

The authors are grateful to Professor Alexey Romanov for help in formulating the problem and interpreting the results.

FUNDING

This research is supported by the grant of Russian Science Foundation №24-12-00229, https://rscf.ru/project/24-12-00229/.

REFERENCES

[1] S.I. Stepanov, V.I. Nikolaev, V.E. Bougrov, A.E. Romanov. Gallium oxide: Properties and applications – a review. *Reviews on Advanced Materials Science*, 2016, vol. 44, pp. 63–86.

[2] T. Igarashi, Y. Ueda, K. Koshi, R. Sakaguchi, S. Watanabe, S. Yamakoshi, A. Kuramata. Growth of 6 inch diameter β-Ga_2O_3 crystal by the vertical Bridgman method. *Physica Status Solidi B*, 2025, vol. 262, no. 8, art. no. 2400444.

[3] K. Adachi, H. Ogi, N. Takeuchi, N. Nakamura, H. Watanabe, T. Ito, Y. Ozaki. Unusual elasticity of monoclinic β-Ga_2O_3. *Journal of Applied Physics*, 2018, vol. 124, no. 8, art. no. 085102.

[4] X.Q. Zheng, H. Zhao, Z. Jia, X. Tao, P.X. Feng. Young's modulus and corresponding orientation in β-Ga_2O_3 thin films resolved by nanomechanical resonators. *Applied Physics Letters*, 2021, vol. 119, no. 1, art. no. 013505.

[5] J.Q. Zhang, H. Zhou, W. Jiang, S.X. Hu, X.P. Ren, C.W. Zhang. Investigation of dynamic mechanical properties and constitutive model of (010) plane of gallium oxide crystals under shock loading. *Ceramics International*, 2022, vol. 48, no. 19, pp. 27823–27835.

[6] Y. Yao, Y. Sugawara, K. Sasaki, A. Kuramata, Y. Ishikawa. Anisotropic mechanical properties of β-Ga_2O_3 single-crystal measured via angle-dependent nanoindentation using a Berkovich indenter. *Journal of Applied Physics*, 2023, vol. 134, no. 21, art. no. 215106.

[7] S. Poncé, F. Giustino. Structural, electronic, elastic, power, and transport properties of β-Ga_2O_3 from first principles. *Physical Review Research*, 2020, vol. 2, no. 3, art. no. 033102.

[8] Y. Li, X. Zhang, M. Liu, L. Shen. A critical review of machine learning interatomic potentials and Hamiltonian. *Journal of Materials Informatics*, 2025, vol. 5, no. 4.

[9] H. Ogi. Resonant Ultrasound Spectroscopy for Measuring of Elastic Constants of Small Solids. *Journal of the Society of Materials Science, Japan*, 2020, vol. 69, no. 8, pp. 582–585.

[10] F.F. Balakirev, S.M. Ennaceur, R.J. Migliori, B. Maiorov, A. Migliori. Resonant ultrasound spectroscopy: The essential toolbox. *Review of Scientific Instruments*, 2019, vol. 90, no. 12, art. no. 121401.

[11] T. Lee, R.S. Lakes, A. Lal. Resonant ultrasound spectroscopy for measurement of mechanical damping: Comparison with broadband viscoelastic spectroscopy. *Review of Scientific Instruments*, 2000, vol. 71, no. 7, pp. 2855–2861.

[12] J. Torres, A. Flores-Betancourt, R.P. Hermann. RUScal: Software for the analysis of resonant ultrasound spectroscopy measurements. *Journal of the Acoustical Society of America*, 2022, vol. 151, no. 5, pp. 3547–3563.

[13] F. Theuss, G.D. Simarro, A. Shragai, G. Grissonnanche, I.M. Hayes, S. Saha, T. Shishidou, T. Chen, S. Nakatsuji, S. Ran, M. Weinert, N.P. Butch, J. Paglione, B.J. Ramshaw. Resonant ultrasound spectroscopy for irregularly shaped samples and its application to uranium ditelluride. *Physical Review Letters*, 2024, vol. 132, no. 6, art. no. 066003.

[14] V.A. Solovyov, I.G. Mikhailov. On the theory of compound piezoelectric vibrator. *Proceedings of the Academy of Sciences of the USSR*, 1956, vol. 20, no. 2, p. 15.

[15] S. Kustov, S. Golyandin, A. Ichino, G. Gremaud. A new design of automated piezoelectric composite oscillator technique. *Materials Science and Engineering: A*, 2006, vol. 442, no. 1–2, pp. 532–537.

[16] V.V. Kaminskii, D.Yu. Panov, V.A. Spiridonov, D.A. Bauman, D.A. Kalganov, M.P. Scheglov, A.E. Romanov. Effect of high-temperature annealing on the internal friction and optical transmittance of single crystal gallium oxide. *Materials Physics and Mechanics*, 2024, vol. 52, no. 5, pp. 48–54.

[17] A. Fernández González, K. Sapozhnikov, P. Pal-Val, S. Kustov. Effect of acoustic oscillations on non-equilibrium state of magnetic domain structure in cubic Ni_2MnGa single crystal. *Materials*, 2023, vol. 16, no. 7, art. no. 2547.

[18] V.D. Natsik, P.P. Pal-Val, S.N. Smirnov. Theory of a compound piezoelectric vibrator. *Russian Ultrasonics*, 1998, vol. 44, no. 5, pp. 553–560.

[19] P. Giannozzi, S. Baroni, N. Bonini, M. Calandra, R. Car, C. Cavazzoni, D. Ceresoli, G.L. Chiarotti, M. Cococcioni, I. Dabo, A. Dal Corso, S. de Girancoli, S. Fabris, G. Fratesi, R. Gebauer, U. Gerstmann, C. Gougoussis, A. Kokalj, M. Lazzeri, L. Martin-Samos et al. QUANTUM ESPRESSO: a modular and open-source software project for quantum simulations of materials. *Journal of Physics: Condensed Matter*, 2009, vol. 21, no. 39, art. no. 395502.

[20] V.V. Kaminskii, D.A. Kalganov, D.I. Panov, V.A. Spiridonov, A.I. Ivanov, M.V. Rozaeva, D.A. Bauman, A.E. Romanov. A study of gallium oxide by using the piezoelectric composite oscillator technique at a frequency of 100 kHz. *Condensed Matter and Interphases*, 2023, vol. 25, no. 4, pp. 548–556.

[21] A. Dal Corso. Elastic constants of beryllium: a first-principles investigation. *Journal of Physics: Condensed Matter*, 2016, vol. 28, no. 7, art. no. 075401.

[22] P.E. Blöchl. Projector augmented-wave method. *Physical Review B*, 1994, vol. 50, no. 24, art. no. 17953.

[23] D. Wu, Y. Yan, X. Sun, X. Gao, D. Liu, Y. Liu, Z. Jin, N. Xia, H. Zhang, D. Yang. Characterization of dislocations in $(\bar{3}10)$ β-Ga_2O_3 single crystal grown by the casting method. *Journal of Alloys and Compounds*, 2025, vol. 1018, art. no. 179092.

[24] Y. Yao, Y. Sugawara, Y. Ishikawa. Identification of Burgers vectors of dislocations in monoclinic β-Ga_2O_3 via synchrotron X-ray topography. *Journal of Applied Physics*, 2020, vol. 127, no. 20, art. no. 205110.

[25] Y. Nishino, H. Ogawa, S. Asano. Mechanical hysteresis due to microplasticity in alumina with microcracks. *Philosophical Magazine Letters*, 1992, vol. 66, no. 6, pp. 313–316.

УДК: 548.4:534.631:620.192.63

Моделирование и анализ механических колебаний в объёмном кристалле оксида галлия

Д.А. Калганов [1,2], В.В. Каминский [1], П.А. Богданов [1], Д.Ю. Панов [1], Д.А. Бауман [1]

[1] Институт перспективных систем передачи данных, Университет ИТМО, Кронверкский пр., 49, литер А, Санкт-Петербург, 197101, Россия

[2] Лаборатория дифракционных методов исследования реальной структуры кристаллов, Физико-технический институт им. А.Ф. Иоффе РАН, Политехническая ул., 26, Санкт-Петербург, 194021, Россия

Аннотация. В данной работе исследуются упругие свойства кристаллов β-фазы оксида галлия с применением метода конечных элементов и метода составного осциллятора. На основе обобщенного градиентного приближения были получены следующие значения упругих постоянных: C_{11} = 250,4 ГПа, C_{12} = 132,3 ГПа, C_{13} = 148,8 ГПа, C_{15} = –19,6 ГПа, C_{22} = 357,1 ГПа, C_{23} = 101,1 ГПа, C_{25} = 16.4 ГПа, C_{33} = 334,5 ГПа, C_{35} = 4,5 ГПа, C_{44} = 64,4 ГПа, C_{46} = 27,2 ГПа, C_{55} = 69,1 ГПа, C_{66} = 99,8 ГПа. Измерения, проведенные при комнатной температуре методом составного осциллятора, показали резонансную частоту 107954 Гц и логарифмический декремент затухания $2{,}59 \cdot 10^{-4}$. Эти данные хорошо согласуются с результатами моделирования методом конечных элементов, согласно которым продольный резонанс должен наблюдаться вблизи частоты 108624 Гц (с учетом принятого коэффициента потерь). Полученные результаты служат научной основой для изучения упругости и микропластичности β-Ga_2O_3 методами акустического резонанса.

Ключевые слова: упругие свойства; метод составного пьезоэлектрического осциллятора; теория функционала плотности; конечно-элементный метод; оксид галлия